

Scaling and scaling crossover for transport on anisotropic fractal structures

A. Adrover

Centro Interuniversitario sui Sistemi Disordinati e sui Frattali nell'Ingegneria Chimica, Dipartimento di Ingegneria Chimica, Università di Roma "La Sapienza," via Eudossiana 18, 00184 Roma, Italy

W. Schwalm

Department of Physics, University of North Dakota, Grand Forks, North Dakota 58202-7129

M. Giona*

Centro Interuniversitario sui Sistemi Disordinati e sui Frattali nell'Ingegneria Chimica, Dipartimento di Ingegneria Chimica, Università di Roma "La Sapienza," via Eudossiana 18, 00184 Roma, Italy

D. Bachand

Department of Electrical Engineering, University of North Dakota, Grand Forks, North Dakota 58202-7165

(Received 15 November 1996)

Diffusion into fibrous anisotropic structures can exhibit a variety of crossover phenomena. Scaling of amount adsorbed versus time in such structures is studied by standard renormalization methods as a function of anisotropy for several kinds of discrete models. Total mass adsorbed as a function of time from a reservoir attached at a single point exhibits different power laws in different logarithmic ranges separated by crossover times. For example, one expects a transition from scaling characteristic of a one-dimensional channel to that of an effective isotropic medium as adsorbed material spreads out over successively longer length scales. In the models studied, there is an easy diffusion pathway imbedded in a medium having a much lower diffusivity. The easy-diffusion subspace can have fractal dimension below that of the background. Different types of crossovers are identified. Power-law exponents for mass sorption are controlled by interplay between effective source dimension and fractal dimension of the active diffusion space. Exponents characterizing scaling of crossover times as a function of anisotropy are largely independent of the fractal dimension of the easy-diffusion pathways. [S1063-651X(97)14506-8]

PACS number(s): 61.43.Hv, 47.53.+n, 47.55.Mh, 51.10.+y

I. INTRODUCTION

Here we analyze difference models for diffusion in a highly anisotropic fractal medium. Simple fractal lattices are used as model structures, in part because they preserve certain aspects of random fractal structures, which are of increasing practical interest [1], and partly because the regular lattices admit an exact analytic treatment. An exact analysis of simple model problems gives insight that is different from that offered by the approximate solution of more realistic problems. Thus we can discover the mechanisms that control scaling of sorption by means of diffusion, and the kinds of transitions that can correspond to scaling crossover.

Consider a fibrous material in which diffusion is fast along the local fiber direction and slow in perpendicular directions. The medium is represented as a fractal network. [2] Diffusion is described using coupled differential equations for the concentration, one equation per lattice point. A microscopic diffusivity is assigned to each of the bonds: unity for fast diffusion, or k for slow diffusion. In typical anisotropic materials, either the material on a gross scale has a preferred diffusion direction or the easy diffusion direction is defined only within domains of a characteristic size. Ori-

tation of different domains can fluctuate randomly, so that gross properties of the medium are isotropic. Even when fibers introduce a preferred direction on all length scales, the sum over diffusion paths can lead to isotropy on all but the shortest scales. In contrast, the models discussed below exhibit effects of anisotropy over arbitrary distances. They might represent long fibers packed within a fractal diffusion space, or leaky pipelines or veins embedded in a porous matrix. For these models the bonds of higher diffusivity form an easy-diffusion subspace that can be either straight or tortuous. We call this the easy subspace for short. Of particular interest are the exponents that characterize the amount of material adsorbed as a function of time, or the crossover time as a function of relative local diffusivities.

Figure 1 shows such a model on a portion of the simple lattice introduced by Dhar [3]. Dashed lines denote bonds of diffusivity k , while solid bonds have unit diffusivity. In this model the easy-diffusion subspace is a Hamiltonian path from one corner to another, visiting each lattice point once.

One can anticipate an interesting crossover phenomenon. Suppose the structure is empty and that at time $t=0$ one end of the easy subspace is connected to a reservoir of material that will diffuse into the lattice. When k is small the easy subspace behaves as a tortuous pipeline that leaks slightly. The diffusing material follows the pipe initially, so the total amount absorbed is proportional to $t^{1/2}$, characteristic of diffusion into a linear chain. The mean invasion distance mea-

*Permanent address: Dipartimento di Ingegneria Chimica, Università di Cagliari, piazza d'Armi, 09123 Cagliari, Italy.

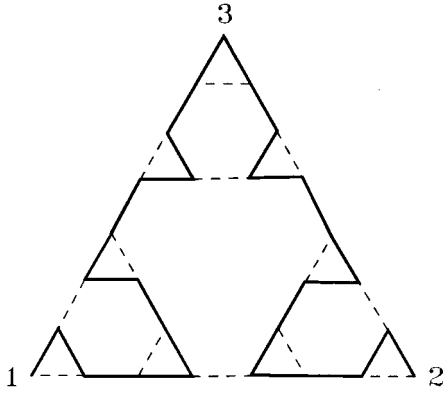


FIG. 1. Anisotropic version of the 3-simplex lattice. Dashed bonds have low diffusivity or high resistance. Solid bonds form a Hamiltonian path.

sured along the pipe (i.e., chemical distance) at time t is thus proportional to $t^{1/2}$. While most of the material follows the pipe at first, a small amount of seepage takes place via the dashed bonds. The amount transported by seepage increases as a higher power of t than does diffusion along the pipeline. Eventually seepage dominates. There is a crossover time t_c before which the amount adsorbed scales as $t^{1/2}$ and after which it scales as some other power of t , characteristic of diffusion into an isotropic simplex with a rescaled effective diffusivity. The crossover time t_c should scale as $k^{-\nu}$ for some crossover exponent ν depending on geometry of the diffusion space.

Adler studied static scaling in an anisotropic fractal lattice model with a macroscopic easy-diffusion direction [2]. The physics of such a model is clearly different from that of the models studied here. Different crossover is expected.

The relation between the difference models considered here and partial differential equations (PDE's) that would apply on a gross scale is not trivial. First, since the diffusion space is fractal, the difference models correspond in no simple way to PDE's, even in the isotropic limit [4,5]. Second, consider a difference model defined on a square lattice with an easy subspace that follows a space-filling curve, visiting each site in an erratic manner. Even in this case when the space is Euclidean, the model becomes equivalent to a PDE for an effective isotropic medium only after the difference equations are renormalized until the rescaled lattice spacing exceeds the crossover length L_c associated with t_c . In fact, each continuum limit corresponds to a renormalization fixed point of the discrete system [6]. In this paper we will regard discrete models as more fundamental than the limiting PDE's.

The continuum diffusion equation relates to the classical wave equation or the Schrödinger equation by a change in time dependence and a change in boundary conditions. Difference schemes for diffusion derived from material conservation and Fick's law define generalized difference Laplacians based on adjacency, rather than distances or angles [4,7]. Thus microscopic diffusion models serve as guides for constructing difference models of vibration or electron propagation.

In the case of vibrations the bonds represent springs and the differential equation at each lattice point describes trans-

verse displacement, rather than change in local concentration. For the Schrödinger equation, the local variables represent probability amplitude. Therefore some results presented here can also be transferred to vibrations or electron propagation, or to models for spin dynamics. For example, Hood and Southern [8] treated spin waves on an anisotropic Sierpinski lattice, much like the one in Fig. 1.

The general scaling theory of diffusion on fractals is reviewed by Havlin and Ben-Avraham [9]. The Green-function methods used below are standard [10,11]. They consist of transfer-matrix renormalization applied to a small set of pivotal Green functions. The application to transport in porous fractal media, including proper treatment of boundary conditions, is worked out in detail by Giona *et al.* [12].

II. STATIC SCALING

Consider the model of Fig. 1. Finding static solutions is equivalent to finding the resistance of a network in which the dashed bonds have resistance $1/k$, and the solid bonds have resistance 1. Basic circuit theory applies. [2] The structure is built up in stages or generations. The generation $n+1$ network is formed by connecting three generation n networks together using two solid bonds and one dashed one. Each part is a triangle characterized electrically by two Y-equivalent resistance parameters r_1 and r_2 . If sites 1 and 2 are base vertices and 3 the top vertex as in Fig. 1, then the resistance from 1 to 2 is $2r_1$ while the resistance from 1 to 3 is r_1+r_2 . By combining resistances in series and parallel, one arrives at a recursion formula giving the corresponding resistances R_1 and R_2 on the next generation in terms of r_1 and r_2 , namely,

$$R_1 = r_1 + \frac{(1+2r_1)(1+2kr_2)}{1+2k+4kr_1+2kr_2},$$

$$R_2 = r_2 + \frac{k(1+2r_1)^2}{1+2k+4kr_1+2kr_2}. \quad (2.1)$$

These recursions comprise a primitive renormalization in that they relate resistances of portions of the structure at different length scales. They are nonlinear difference equations which decouple because they commute with the Lie group [13,14] generated by

$$\mathcal{L} = \left(\frac{1}{2} + r_1\right) \frac{\partial}{\partial r_1} + \left(\frac{1}{2k} + r_2\right) \frac{\partial}{\partial r_2}. \quad (2.2)$$

Transforming to canonical variables,

$$u = \frac{-(1-k-2kr_1+2kr_2)}{2k(1+2r_1)},$$

$$v = \ln\left(\frac{1}{2} + r_1\right), \quad (2.3)$$

recursion Eqs. (1) decouple to

$$\begin{aligned} U &= u - \frac{4(1-u)u}{5-6u}, \\ V &= v + \ln\left(\frac{2+3u}{2+u}\right). \end{aligned} \quad (2.4)$$

Numerical values of r_1 and r_2 for a given k and generation number n are found easily by iterating Eqs. (2.1), starting from $r_1=r_2=0$ for a single point. To analyze the diffusion crossover and obtain the scaling exponent ν it is more convenient to use Eqs. (2.4). There is an unstable fixed point at $u=0$ with multiplier 3 and a stable fixed point at $u=1$ with multiplier $\frac{1}{5}$. These correspond, respectively, to resistance scaling proportional either to the length of the easy subspace or to the resistance of an isotropic Sierpinski network $\sim(\frac{5}{3})^n$. In the framework of diffusion, these behaviors describe scaling of the total amount absorbed before and after the crossover from transport along the pipe to transport by seepage.

To compute the crossover time t_c , suppose k is small, so the initial value $u_0=2k/(1+k)$ is near $u=0$. The crossover takes place when u makes the transit from the neighborhood near 0 to the vicinity of 1, which is a rather abrupt transition. Thus to find t_c we first compute the generation number n at which $u=\frac{1}{2}$ for a given k value. Since the length of the easy subspace is 3^n , we associate this with the distance diffused along an equivalent one-dimensional chain. Using the solution for diffusion on a linear chain, we have $t_c^{1/2} \sim 3^n$ or $t_c \sim 9^n$. All that remains is to find n at which $u=\frac{1}{2}$.

Using undetermined coefficients [15], we develop the Poincaré series at the unstable point

$$u(s) = \sigma + \frac{\sigma^2}{6} - \frac{\sigma^3}{144} + O(\sigma^4), \quad (2.5)$$

where $\sigma = \sigma_0(k)3^n$ with $\sigma_0(k) = 2k - 8k^2/3 + \dots$. Using the expansion Eq. (2.5) in conjunction with the recursion Eqs. (2.4) we can solve $u(\sigma_*) = \frac{1}{2}$ to obtain $\sigma_* = 0.873361$. This gives

$$t_c = \left(\frac{1}{4k^2} + \frac{2}{3k} + \dots \right) \sigma_*^2. \quad (2.6)$$

Apparently the crossover exponent in this case is $\nu=2$.

Now consider another model which will lead to a different crossover exponent. Imagine a similar 2-simplex structure with bond strengths allotted differently as in Fig. 2. In the circuit analogy the solid and dashed lines have resistances 1 and $1/k$ as before. The easy diffusion space is the base line, so that as $k \rightarrow 0$ the resistance becomes 2^n . In the isotropic limit $k \rightarrow 1$ the resistance becomes $(\frac{5}{3})^n$.

To construct the generation $n+1$ lattice requires two different building blocks, two copies of the generation n lattice form the base, while the upper block is generation n of an isotropic lattice with uniform bond resistance $1/k$. Thus the recursion relations involve three quantities, the Y -parameter resistances r_1 and r_2 defined as above and the corresponding

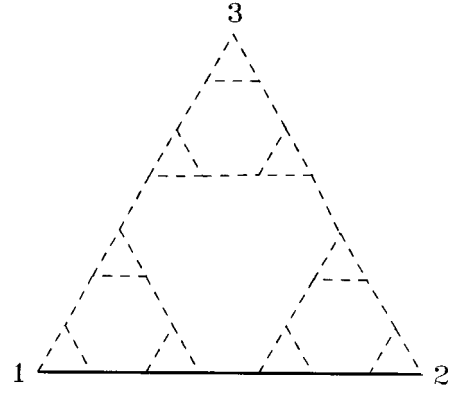


FIG. 2. Anisotropic 3-simplex with easy diffusion along the baseline.

r_0 for the isotropic part. Intuition suggests that the r_0 recursion should decouple, and indeed it does. From basic circuit theory,

$$R_0 = r_0 + \frac{1+2kr_0}{3k},$$

$$R_1 = r_1 + \frac{(1+2r_1)(1+kr_0+kr_2)}{2+k+2kr_0+2kr_1+2kr_2},$$

$$\begin{aligned} R_2 &= (1+4kr_0+k^2r_0+3k^2r_0^2+2k^2r_0r_1+2kr_2+4k^2r_0r_2 \\ &\quad +k^2r_2^2)[k(2+k+2kr_0+2kr_1+2kr_2)]^{-1}. \end{aligned} \quad (2.7)$$

Again the recursions commute with a Lie group,

$$\mathcal{L} = \left(\frac{1}{2k} + r_0 \right) \frac{\partial}{\partial r_0} + \left(\frac{1}{2} + r_1 \right) \frac{\partial}{\partial r_1} + \left(\frac{1}{2k} + r_2 \right) \frac{\partial}{\partial r_2}, \quad (2.8)$$

with canonical variables

$$\begin{aligned} a &= \frac{2k}{1+2kr_0}, \\ u &= \frac{k(1+2r_1)}{1+2kr_0}, \\ v &= \frac{1+2kr_1}{1+2kr_0}, \end{aligned} \quad (2.9)$$

in terms of which the recursion Eqs. (2.7) become

$$A = \frac{3a}{5},$$

$$U = \frac{3u(2+u+2v)}{5(1+u+v)}, \quad (2.10)$$

$$V = \frac{3(3+2u+4v+v^2)}{10(1+u+v)}.$$

Thus the variable a is completely decoupled and no longer enters the u and v recursions. The latter have three impor-

tant fixed points: an inaccessible source at (0,0), a saddle at $(0, \frac{9}{7})$, which controls the crossover, and a sink at (1,1) representing the large-scale, isotropic effective-medium limit. By linearizing near the saddle we can expand u and v in terms of scaling variables σ and τ such that

$$u(\sigma, \tau) = 3\tau - \frac{315\tau^2}{32} + \frac{11025\tau^2(11\sigma + 272\tau)}{90112} + \dots,$$

$$v(\sigma, \tau) = \frac{9}{7} - \sigma - \tau + \frac{2205\tau^2}{608} + \frac{1575(49\sigma - 752\tau)\tau^2}{90112} + \dots, \quad (2.11)$$

where $a = a_0(k)(\frac{3}{5})^n$, $\sigma = \sigma_0(k)(\frac{3}{10})^n$, and $\tau = \tau_0(k)(\frac{6}{5})^n$. The initial values are

$$a_0 = 2k, \quad u_0 = k, \quad v_0 = 1. \quad (2.12)$$

When k is small, τ and a are initially small and σ is initially large, and one finds the initial behaviors

$$r_0 = \frac{1}{2k} \left[\left(\frac{3}{5} \right)^n - 1 \right],$$

$$r_1 \sim \frac{1}{2} (2^n - 1), \quad (2.13)$$

$$r_2 \sim \frac{1}{6} \left[2^n - \left(\frac{1}{2} \right)^n \right] + \frac{1}{k} \left[\frac{9}{14} \left(\frac{5}{3} \right)^n - \frac{1}{7} \left(\frac{1}{2} \right)^n - \frac{1}{2} \right],$$

so that r_1 increases in proportion to the length of the base, and r_2 increases as in the isotropic fractal. After crossover, τ becomes large and σ small. The trajectory in (u, v) tends to the sink representing isotropic scaling, near which r_0 , r_1 and r_2 each tend to the same limiting form $(7k/6)(\frac{5}{3})^n$. This indicates an effectively isotropic fractal medium with local diffusivity $7k/6$. The crossover occurs when (u, v) is closest to the saddle. The simplest definition of crossover is the criterion $\sigma = \tau$. Thus one has $\sigma_0(k)(\frac{3}{10})^n = \tau_0(k)(\frac{6}{5})^n$ or $\tau_0(k)/\sigma_0(k) = 4^n$. If k is small enough so mass uptake before crossover is as for a linear chain, then $t_c = L^2 = 4^n$, so that

$$t_c = \frac{3}{2k}. \quad (2.14)$$

For this model, the exponent is $\nu = 1$ as opposed to $\nu = 2$ for the model of Fig. 1.

In fact diffusion into the structure of Fig. 2 exhibits more complicated scaling transitions, as discussed below where we consider adsorption as a function of time. When k is small enough so that the easy subspace along the backbone saturates before the crossover time Eq. (2.14), there is a transition to scaling characteristic of the isotropic fractal attached to a reservoir, not by a point, but along the entire base line. The base line acts as a line source. On the other hand, if crossover occurs before saturation of the base line, the intermediate scaling is characteristic of a mixed state. Thus there will be two transition times in the latter case.

III. DIFFUSION INCLUDING TIME DEPENDENCE

An outline of methods used is given here. Details are presented in Ref. [12]. The discrete diffusion equation is

$$\frac{d}{dt} c_i(t) = \sum_j k_{ij} [c_j(t) - c_i(t)] + f_i(t), \quad (3.1)$$

where k_{ij} is 1 for solid bonds, and k for dashed bonds; otherwise it is zero. The source term $f_i(t)$ is included for generality. Equation (3.1) assumes conservation of material, as is appropriate for a closed system. Summing on i shows that the time rate of change of the sum of all concentrations is just the sum of the source terms. When there are no sources or sinks, material is conserved. It is convenient to rewrite the system in vector matrix form

$$\frac{d}{dt} c(t) - Hc(t) = f(t), \quad (3.2)$$

where H is explicitly mass conserving:

$$H_{ij} = k_{ij} - \delta_{ij} \sum_n k_{in}. \quad (3.3)$$

We will analyze diffusion into the structure assuming zero initial concentration. A reservoir of concentration c_0 is attached via a bond of unit diffusivity to site 1 located at one end of the easy subspace. The term to be added to the right side of Eq. (3.1) is then $\delta_{i1}[c_0 - c_i(t)]$. Let the reservoir part be incorporated as a source term, $f_i(t) = \delta_{i1}c_0$, while the rest is viewed as resulting from a perturbation of H , namely, V , where $V_{i,j} = -\delta_{i1}\delta_{j1}$. Thus taking Laplace transforms we have the matrix equation

$$(s - H - V)\hat{c}(s) = \hat{f}(s) + c(0). \quad (3.4)$$

Thus

$$\hat{G}^{(d)}(s) = (s - H - V)^{-1} \quad (3.5)$$

defines a set of Green functions such that the Laplace transformed concentration on site i is given by $\hat{c}_i(s) = \sum_j \hat{G}_{ij}^{(d)}(s) \hat{f}_j(s)$.

The quantity of interest is the (sorption) ratio $M(t)/M_\infty$ of material adsorbed at time t to material adsorbed at saturation [16]. If N is the number of lattice sites, then $M_\infty = c_0 N$. The time rate of increase of $M(t)$ is just the rate at which material flows in across the bond of unit diffusivity connecting site 1 to the reservoir. Thus $dM(t)/dt = c_0 - c_1(t)$. In the Laplace domain,

$$\frac{\hat{M}(s)}{M_\infty} = \frac{1}{Ns^2} [1 - \hat{G}_{11}^{(d)}(s)]. \quad (3.6)$$

Therefore, to study scaling with time of the sorption ratio for material entering at a single point, it is only necessary to study scaling of $1 - \hat{G}_{11}^{(d)}(s)$ with s . When diffusion of material into the structure is governed by a power law in time, this corresponds to a straight-line segment in the log-log graph of $1 - \hat{G}_{11}^{(d)}(s)$ versus s . For power-law scaling,

$1 - \hat{G}_{11}^{(d)}(s) \sim s^\beta$ implies $M(t)/M_\infty \sim t^{1-\beta}$. We solve for the Green functions in two separate steps. First we construct recursion relations for the Green functions $\hat{G}_{ij}(s)$ for the closed system. These are defined by

$$\hat{G}(s) = (s - H)^{-1}. \quad (3.7)$$

Then from the matrix Eqs. (3.5) and (3.7) and the definition of the sparse matrix V , one has

$$\hat{G}_{11}^{(d)}(s) = \hat{G}_{11}(s) / [1 + \hat{G}_{11}(s)]. \quad (3.8)$$

Recursion relations are developed for a minimum necessary set of pivotal Green functions. This is the smallest set for which recursions can be written. Both the strategy and the form of the recursions (systems of rational functions) are much the same as in the resistance network examples of Sec. II.

Consider the model of Fig. 1, with lower corner sites 1 and 2 and the upper corner 3 as shown. At generation n of the construction the pivotal set contains the Green functions (x, y, u, v) defined by $x = \hat{G}_{11}(s)$, $y = \hat{G}_{21}(s)$, $u = \hat{G}_{33}(s)$, and $v = \hat{G}_{31}(s)$. Recall that generation $n+1$ is made by assembling three generation n blocks, properly reoriented, and then connecting them together with appropriate bonds.

Let matrix A be the direct sum with diagonal blocks consisting of three copies of the H matrix for generation n , and let matrix B provide the three bonds and adjustments of the diagonal elements necessary to make the connections. If matrix C represents H for generation $n+1$, then $C = A + B$. Green functions (x, y, u, v) of generation n are entries of $\hat{G}_{(n)} = (s - A)^{-1}$, and the corresponding Green functions (X, Y, U, V) for generation $n+1$ are entries of $\hat{G}_{(n+1)} = (s - C)^{-1}$. By matrix manipulation one has the Dyson equation

$$\hat{G}_{(n+1)} = \hat{G}_{(n)} + \hat{G}_{(n)} B \hat{G}_{(n+1)}. \quad (3.9)$$

Because B is sparse, Eq. (3.9) leads directly to recursion formulas for (X, Y, U, V) in terms of (x, y, u, v) . However the formulas are rather long, and they simplify quite a bit if we transform to symmetry-adapted variables with the relative diffusivity scaled out, namely,

$$p = x + y, \quad q = x - y, \quad r = ku, \quad w = \sqrt{kv}. \quad (3.10)$$

Then the recursions become

$$\begin{aligned} P &= q + \frac{(p-q)(1+p+q)}{2+3p+q}, \\ Q &= q + \frac{(1+2q)(p-q+2pr-2qr-4w^2)}{2+p+3q+4r+2pr+6qr-4w^2}, \\ R &= r - \frac{4w^2}{2+3p+q}, \\ W &= \frac{(p-q)w}{2+3p+q}. \end{aligned} \quad (3.11)$$

One can obtain exact numerical results by iterating either the full dynamical system for (x, y, u, v) or else the simpler

Eqs. (3.11) for (p, q, r, w) . In this way we study scaling and crossover for the models of Sec. II as well as the mixed model introduced below. However, it is interesting that the dynamical system of Eqs. (3.11) commutes with the two-parameter, Abelian Lie group generated by

$$\begin{aligned} \mathcal{L}_1 &= \left(\frac{1}{2} + p\right) \frac{\partial}{\partial p} + \left(\frac{1}{2} + q\right) \frac{\partial}{\partial q} - \left(\frac{1}{2} + r\right) \frac{\partial}{\partial r}, \\ \mathcal{L}_2 &= \left(\frac{1}{2} + p\right) \frac{\partial}{\partial p} + \left(\frac{1}{2} + q\right) \frac{\partial}{\partial q} + \left(\frac{1}{2} + r\right) \frac{\partial}{\partial r} + w \frac{\partial}{\partial w}, \end{aligned} \quad (3.12)$$

and so the order reduces [13,14]. To effect this reduction the recursions are expressed in terms of canonical variables of the group. Construction of canonical variables for a two-parameter group is discussed in Ref. [17], pp. 155–165 and Ref. [18], Chap. 7. For the generators, Eqs. (3.12), one can use

$$\begin{aligned} a &= \frac{4w^2}{(1+2p)(1+2r)}, \\ b &= \frac{1+2q}{1+2p}, \\ c &= \ln\left(\frac{1+2r}{2w}\right), \\ d &= \ln(w). \end{aligned} \quad (3.13)$$

Transforming to these variables, the recursions finally become

$$\begin{aligned} A &= \frac{a(1-b)^2}{(3-4a+b)(1+3b)}, \\ B &= \frac{b(3+b)(3-6a+b)}{(1+3b)(1-2a+3b)}, \\ C &= c + \ln\left(\frac{3-4a+b}{1-b}\right), \\ D &= d + \ln\left(\frac{1-b}{3+b}\right), \end{aligned} \quad (3.14)$$

so that the equations for c and d have decoupled. This facilitates an analysis of the scaling properties. A comprehensive discussion of the group theoretic method of reducing lattice problems of this sort will be given elsewhere [19]. The existence of one symmetry in the case of resistance recursions is guaranteed by the fact that when each resistor in a network is scaled by a given factor, the network resistance scales by the same factor. For the analysis below we can simply make use of the reduction Eqs. (3.14) that results from introducing new coordinates, Eqs. (3.13).

IV. SORPTION BEHAVIOR

In each case discussed so far, material diffuses in from a reservoir or source attached at a single site. For interpreting the curves presented below, it is useful to look at a more general source geometry.

When the structure is fed from an arbitrary set \mathcal{B} of sites in contact with an external reservoir, the generalization of Eq. (3.6) is [12]

$$\frac{\hat{M}(s)}{M_\infty} = \frac{N_B}{s^2 N} \left[1 - \frac{1}{N_B} \sum_{i,j \in \mathcal{B}} \hat{G}_{ij}^{(d)} \right] = \frac{N_B}{s^2 N} \Psi(s), \quad (4.1)$$

where N_B is the number of sites in the source \mathcal{B} , and N the total number of sites. The function $\Psi(s)$ generalizes $1 - \hat{G}_{11}^{(d)}(s)$, so that for a single input Eq. (4.1) reduces to Eq. (3.6). A pertinent result obtained in [12] is that when a given structure is fed from different inlet configurations, i.e., from different \mathcal{B} sets, the scaling exponent β associated with $\Psi(s)$ can be different. Recall that $M(t)/M_\infty \sim t^{1-\beta}$. The exponent β will depend in particular on the dimension of \mathcal{B} and on the structure as a whole.

For very short times or large s , diffusion into the structure is linear, being limited by the inlet bond diffusivity. This is an artifact of the discrete nature of the models. For anisotropic models, the amount diffusing into the easy diffusion subspace at somewhat longer times from a source attached to one end scales as $t^{1/2}$ characteristic of a linear chain. Thus in such a case, the log of $\Psi(s)$ is first zero for large $\ln s$ (which we will ignore), then proportional to $(\ln s)/2$ for somewhat lower $\ln s$ before crossing over into other behaviors. At very long times the structure saturates, so that at very negative $\ln s$, the log of $\Psi(s)$ becomes linear in $\ln s$. We will ignore the saturation limit also. These extreme limiting behaviors are not of primary concern. We concentrate on intermediate values of s where fractal scaling can occur. A discussion of which values of s are considered intermediate is found in Ref. [12].

The scaling of $\Psi(s)$ for intermediate values of s for an isotropic lattice with general source configuration \mathcal{B} is summarized by

$$\Psi(s) \sim s^\beta = s^{1-(d_f - d_f^B)/d_w}, \quad (4.2)$$

d_f and d_w being the fractal and walk dimensions [9], respectively, and d_f^B is the fractal dimension of \mathcal{B} . This scaling law also proves to be useful for understanding diffusion into anisotropic models, even when the input is from a single point.

Consider first the behavior of $1 - \hat{G}_{11}^{(d)}(s)$ vs s , as shown in Fig. 3 for the model of Fig. 2 fed from site 1. When $k=0$ the exponent β is $\frac{1}{2}$, as expected for the linear chain. For $k=1$, $\beta = 1 - d_f^S/d_w^S = 0.318$, where $d_f^S = \ln 3/\ln 2 = 1.585$ and $d_w^S = \ln 5/\ln 2 = 2.322$ are the fractal and walk dimensions of the isotropic simplex lattice. This is the expected behavior for an isotropic lattice fed from a corner site. For intermediate values of k (from 10^{-14} to 10^{-2}), a complex crossover behavior occurs due to the presence of the easy subspace, which controls the scaling for large s .

Three different scaling behaviors can be identified in Fig. 3, each with a characteristic β . For small s , the exponent is $\beta_1 = \frac{1}{2}$, as expected. For large s , $\beta_3 = 1 - (d_f^S - 1)/d_w^S$, because the easy subspace saturates and acts as a line source ($d_f^B = 1$), feeding the rest of the structure. In the middle region there is another exponent β_2 which will be discussed presently. Notice from the figure that the extent of the central scaling region depends on the value of k .

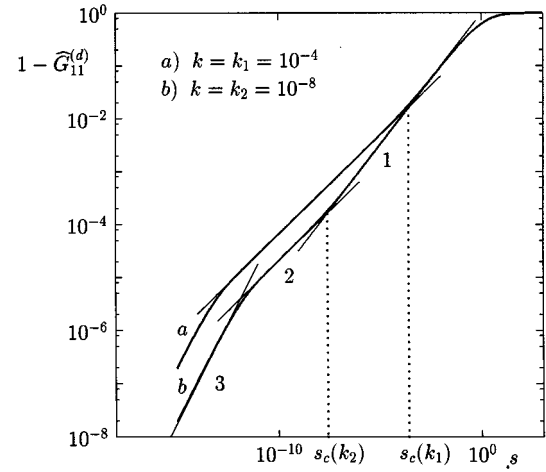


FIG. 3. Log-log plot of $1 - \hat{G}_{11}^{(d)}(s)$ vs s for two different values of the bond diffusivity k , for the anisotropic model of Fig. 2 (order of generation $n = 18$, $N = 3^{18}$). Lines 1, 2, and 3, respectively, show the three theoretical power laws $1 - \hat{G}_{11}^{(d)}(s) \sim s^\beta$, with $\beta = \beta_1$, β_2 , and β_3 . The two vertical dotted lines identify the crossover values s_c , for the two k values.

A similar analysis holds for a family of other anisotropic lattices, such as the one shown in Fig. 4, in which the easy subspace is itself a fractal in the form of a Weierstrass curve with a fractal dimension between 1 and d_f^S . We can think of it as a subfractal or relative fractal. For the model of Fig. 3 the easy subspace dimension is $d_f^B = \ln 12/\ln 8 = 1.195$.

From Fig. 5 we see that, for intermediate values of k , a crossover occurs similar to the one in the scaling for the model of Fig. 2. The exponents are $\beta_1 = \frac{1}{2}$; β_2 , to be discussed in the remainder of this section; and $\beta_3 = 1 - (d_f^S - d_f^B)/d_w^S$, exactly as expected for an isotropic simplex fed from the saturated easy subspace, which acts as a source \mathcal{B} of dimension d_f^B .

Now consider the middle scaling regions with exponents labeled by β_2 for both anisotropic models of Figs. 2 and 4.

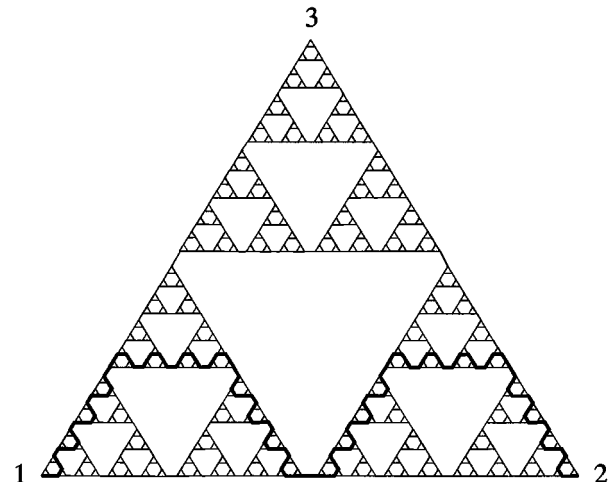


FIG. 4. Anisotropic Sierpinski gasket with strong bonds (diffusivity 1) distributed on a Weierstrass-like curve with fractal dimension $d_f^B = \ln(12)/\ln(8)$.

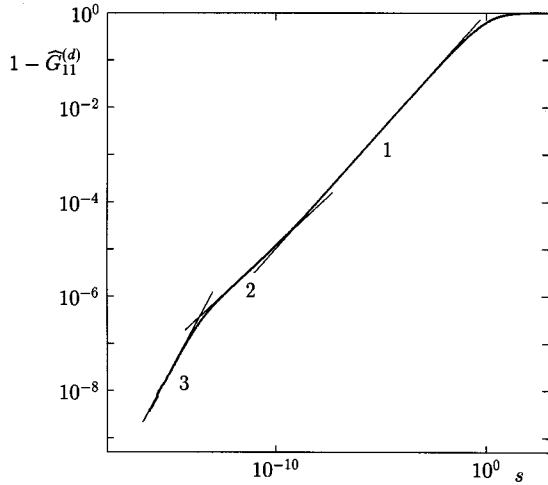


FIG. 5. Log-log plot of $1 - \hat{G}_{11}^{(d)}(s)$ vs s for the anisotropic model of Fig. 4 (generation $n=18$, $k=10^{-10}$). Lines 1, 2, and 3, respectively show theoretical power laws with $\beta=\beta_1$, β_2 , and β_3 .

This is the region corresponding to time scales over which seepage diffusion dominates, although the easy diffusion subspace has not saturated. In this range the scaling exponent is $\beta_2=\beta_1\beta_3$. That this should generally be the case can be seen from the following argument.

Consider the equivalent model of Fig. 6, comprising a simplex with all bonds at diffusivity k , connected to a one-dimensional line with bonds of diffusivity $1-k$, fed by site 1. Bonds connecting sites on the simplex baseline to the external line have diffusivity $g \gg 1$.

Let $\hat{q}_i(s)$ and $\hat{c}_i(s)$, respectively, be the concentrations in the simplex subgraph and in the one-dimensional line of Fig. 6. It follows that

$$\hat{q}_i(s) = \sum_{j \in \mathcal{B}} \hat{G}_{ij}^*(s; k, g) g \hat{c}_j(s), \quad (4.3)$$

where $i=1, \dots, N_{\mathcal{B}}$ are the sites on the baseline of the simplex sublattice and $\hat{G}_{ij}^*(s; k, g)$ is a Green function of the simplex with bond diffusivity k and the boundary \mathcal{B} connected by bonds of strength g to the auxiliary line.

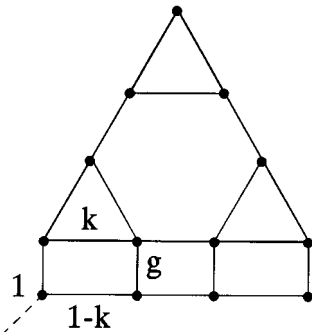


FIG. 6. Schematic representation of a model equivalent to the anisotropic structure in Fig. 2.

It is shown in Ref. [12] that the scaling exponent of the function

$$\Psi_S(s; k, g) = 1 - \frac{1}{N_{\mathcal{B}}} \sum_{i \in \mathcal{B}} \sum_{j \in \mathcal{B}} \hat{G}_{ij}^*(s; k, g) g \sim s^{1 - (d_f^S - 1)/d_w^S} \quad (4.4)$$

is independent of the values of $g > 0$ and $k > 0$.

Since we are interested in the net transfer of material between the two sublattices, when the concentration inside the simplex subgraph is much smaller than the concentration in the line, a reasonable approximation is to assume the transfer rate between the sites on the external line and the simplex baseline is uniform, and can be described by a position-independent effective transfer function $K_{\text{eff}}(s)$,

$$\hat{c}_i(s) - \hat{q}_i(s) = K_{\text{eff}}(s) \hat{c}_i(s). \quad (4.5)$$

This assumption should be justified since, for large g and small k , the main contribution to transfer between site i on the extra line and the adjacent site on the simplex occurs through the bond connecting them directly. The contribution from other paths can be regarded as a uniform perturbation to this main term. The effective transfer rate $K_{\text{eff}}(s)$ in Eq. (4.5) is obtained by averaging over all the transfer sites,

$$K_{\text{eff}}(s) = \frac{\langle \hat{c}_i - \hat{q}_i \rangle}{\langle \hat{c}_i \rangle} = \frac{\langle \hat{c}_i \rangle - \left\langle \sum_j \hat{G}_{ij}^* g \hat{c}_j \right\rangle}{\langle \hat{c}_i \rangle}. \quad (4.6)$$

The position independence of $K_{\text{eff}}(s)$ implies that the quantities \hat{G}_{ij}^* and \hat{c}_i are uncorrelated, $\langle \hat{G}_{ij}^* \hat{c}_j \rangle \approx \langle \hat{G}_{ij}^* \rangle \langle \hat{c}_j \rangle$. Making this decoupling in Eq. (4.6), it follows that

$$\begin{aligned} K_{\text{eff}}(s) &= 1 - \left\langle \sum_j \hat{G}_{ij}^* g \right\rangle \\ &= 1 - \frac{1}{N_{\mathcal{B}}} \sum_{i \in \mathcal{B}} \sum_{j \in \mathcal{B}} \hat{G}_{ij}^* g = \Psi_S(s; k, g). \end{aligned} \quad (4.7)$$

Substituting Eqs. (4.5) and (4.7) into the balance equation for \hat{c}_i ,

$$\begin{aligned} s \hat{c}_i &= \sum_j H_{ij} \hat{c}_j + \delta_{i1} c_0 - g (\hat{c}_i - \hat{q}_i) \\ &= \sum_j H_{ij} \hat{c}_j + \delta_{i1} c_0 - g \Psi_S(s; k, g) \hat{c}_i. \end{aligned} \quad (4.8)$$

Therefore, net diffusion of material between sublattices reduces to a diagonal term in the equations for \hat{c}_i ,

$$\hat{c}_i = \hat{G}_{i1}^{(d,L)}(s + g \Psi_S(s; k, g)), \quad (4.9)$$

where the superscript (L) indicates the Green functions for the extra line subgraph, and so the overall transfer of material into the system is controlled by the composite function

$$1 - \hat{G}_{11}^{(d)}(s) = 1 - \hat{G}_{11}^{(d,L)}(s + g \Psi_S(s; k, g)). \quad (4.10)$$

According to Eq. (4.10), the scaling behavior divides into three regions. For s close to zero,

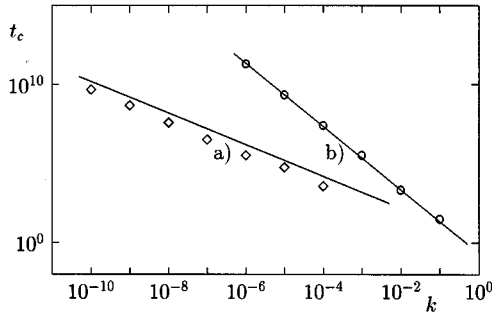


FIG. 7. Crossover time t_c vs bond diffusivity k for the two anisotropic models of Figs. 1 (\diamond) and 2 (\circ). Lines represent the theoretical predictions obtained from the static scaling of resistances (line a) (2.14) and (line b) (2.6).

$s < g \Psi_S(s; k, g) \sim s^{1 - (d_f^S - 1)/d_w^S}$, $\hat{G}_{11}^{(d,L)}(s) \sim s$, and therefore $1 - \hat{G}_{11}^{(d)}(s) \sim s^{1 - (d_f^S - 1)/d_w^S}$, corresponding to line 3 in Fig. 3. With increasing s , $1 - \hat{G}_{11}^{(d,L)}(s) \sim s^{1/2}$, which implies that $1 - \hat{G}_{11}^{(d)}(s) \sim s^{[1 - (d_f^S - 1)/d_w^S]/2}$, which explains the scaling exponent β_2 the region 2 of Fig. 3, i.e., $\beta_2 = \beta_1 \beta_3$. If we increase s further, then $\Psi_S(s; k, g) \sim 1$, and therefore $1 - \hat{G}_{11}^{(d)}(s) \sim s^{1/2}$, corresponding to $\beta_1 = 1/2$ in Fig. 3. This analysis explains all the crossovers of $1 - \hat{G}_{11}^{(d)}(s)$ observed in Fig. 3 (see also Figs. 7 and 8).

Now consider the time $t_c = 1/s_c$ for crossover between the diffusion within the easy subspace (slope β_1 in Figs. 3 and 5) and the seepage transport regime (slope β_2 in Figs. 3 and 5). This transition is defined by the elbow at $s_c(k)$, as is indicated by dotted lines in Fig. 3 for two k values. It is straightforward to study $s_c(k)$ and hence $t_c(k)$ numerically as a function of k . When we graph $\ln t_c$ versus $\ln k$ for the model of Fig. 1 we find a straight line, as expected. The slope and intercept agree with the values of the exponent $\nu = 2$ and the prefactor shown in the asymptotic expansion Eq. (2.6). A

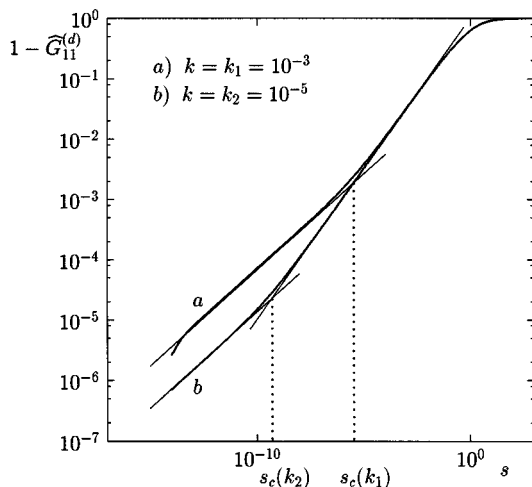


FIG. 8. Log-log plot of $1 - \hat{G}_{11}^{(d)}(s)$ vs s for the anisotropic model of Fig. 1. The two vertical dotted lines identify the crossover values s_c , for the two k values.

similar graph for the model of Fig. 2 gives a line with slope $\nu = 1$, in agreement with the estimate Eq. (2.14). However the prefactor $\frac{3}{2}$ in Eq. (2.14) does not quite fit numerical results. We expect that a definition of crossover more sophisticated than $\sigma = \tau$ is necessary.

V. CONCLUSION

The models presented are microscopically anisotropic, and are chosen so that the easy subspace forms a long, continuous diffusion pathway. This is not the most general situation, or even the most common one. It is apt to occur in crushed fibrous materials. More commonly, one might find either a macroscopic easy-diffusion direction or else bundles of short, locally parallel fibers occurring in randomly oriented domains. The latter morphology is reasonably represented as bundles of randomly oriented tubules, and it behaves as a homogeneous effective medium on all but the shortest length scales. However, in the case of a continuous easy-diffusion subspace we have seen that interesting crossover behaviors are possible. When the effective dimensionality of the easy subspace is less than that of the porous space as a whole, these crossovers arise due to competition between higher local diffusivity and a growing number of shorter diffusion paths. If there is a large difference between the filling time for the easy subspace and the final saturation time, the easy subspaces can behave as a distributed source, giving rise to other crossover phenomena.

Such crossover scaling is also expected in nonfractal structures, which have a similar type of easy-diffusion subspace. The simplest example is the case of a long blood vessel or a long, one-dimensional pipeline embedded in a slightly porous matrix. If the matrix is two dimensional, for example, then resistance to seepage through the background matrix increases logarithmically with length, while resistance to transport by diffusion along the pipeline increases linearly. There will be a crossover from linear diffusion to seepage at a time that depends in a nonalgebraic way on the seepage diffusivity. In the fractal model of Fig. 2, the time to cross over from linear diffusion to seepage scales as the reciprocal of the seepage diffusivity, while for the space-filling easy subspace shown in Fig. 1, the crossover time scales as the inverse square of the seepage diffusivity, so that the exponent is $\nu = 2$. From numerical iteration of the relevant recursion relations, one also finds $\nu = 2$ in cases with subfractal easy subspace. In particular, the exponent ν does not depend on fractal dimensions.

The power-law exponent β for the time dependence of the net amount adsorbed has an interesting product form for times after crossover to seepage dominated diffusion, but before saturation of the easy subspace. In Sec. IV this was shown to correspond to a position-independent effective transfer rate between the easy subspace and the background.

In strongly inhomogeneous and anisotropic media, time scales are set by competing processes. For the most part, the corresponding exponents do not characterize universal classes. The results of the current study demonstrate several competing transport mechanisms, and show analytically what kinds of time dependences can result. For extremely anisotropic morphologies treated in this work it is not cor-

rect, for example, to apply an effective-medium approximation until diffusion has spread material over distances exceeding a correlation length which depends on the degree of anisotropy. Fortunately these distances may not be long for many systems of interest.

ACKNOWLEDGMENT

This work was supported in part by NATO CRG941289. The participation of D.B. was made possible by a REU stipend from NDEPSCoR.

-
- [1] *Chaos and Fractals in Chemical Engineering*, edited by G. Biardi, M. Giona, and A. R. Giona (World Scientific, Singapore, 1995) .
- [2] P. M. Adler, *Porous Media: Geometry and Transports* (Butterworth-Heinmann, Washington, DC, 1992).
- [3] D. Dhar, *J. Math Phys.* **18**, 577 (1977); **19**, 5 (1978).
- [4] J. Kigami, *Jpn. J. Appl. Math.* **6**, 259 (1989); *Trans. Am. Math. Soc.* **335**, 721 (1993); J. Kigami and M. Lapidus, *Commun. Math. Phys.* **158**, 93 (1993).
- [5] H. E. Roman and M. Giona, *J. Phys. A* **25**, 2107 (1992).
- [6] J.B. Kogut, *Rev. Mod. Phys.* **51**, 659 (1979).
- [7] M. Giona, in *Fractals in Natural and Applied Sciences*, edited by M. M. Novak (Elsevier, Amsterdam, 1994), p. 153; *Chaos and Fractals in Chemical Engineering* (Ref. [1]), p. 3.
- [8] M. Hood and B. W. Southern, *J. Phys A* **19**, 2679 (1986).
- [9] S. Havlin and D. Ben-Avraham, *Adv. Phys.* **37**, 695 (1987).
- [10] W. A. Schwalm and M. K. Schwalm, *Phys. Rev. B* **37**, 9524 (1988).
- [11] V. Sivan and R. Blumenfeld *et al.*, *Europhys. Lett.* **7**, 249 (1988).
- [12] M. Giona, W. A. Schwalm, M. K. Schwalm, and A. Adrover, *Chem. Eng. Sci.* **51**, 4717 (1996); **51**, 4731 (1996); **51**, 5065 (1996).
- [13] S. Maeda, *Math. Japonica* **25**, 405 (1980); *IMA J. Appl. Math.* **35**, 129 (1987).
- [14] G. Quispel and X. Sahadevan, *Phys. Lett. A* **184**, 64 (1993).
- [15] T. Saaty, *Modern Nonlinear Equations* (Dover, New York, 1981), p. 178ff.
- [16] J. Crank, *The Mathematics of Diffusion* (Clarendon, Oxford, 1975).
- [17] A. Cohen, *Introduction to the Lie Theory of One-Parameter Groups* (Heath, New York, 1911).
- [18] H. Stephani, *Differential Equations and their Integration Using Symmetry* (Cambridge University Press, Cambridge, 1989).
- [19] W. A. Schwalm, M. K. Schwalm, and M. Giona, this issue, *Phys. Rev. E* **55**, 6741 (1997).